Inorg. Chem. **2004**, *43*, 5080–5085

Electrochemical Determination of Triple Helices: Electrocatalytic Oxidation of Guanine in an Intramolecular Triplex

Rebecca C. Holmberg and H. Holden Thorp*

Department of Chemistry, University of North Carolina at Chapel Hill, Chapel Hill, North Carolina 27599-3290

Received January 27, 2004

Electrocatalytic oxidation of the oligonucleotide 5′- GAA GAG GTT TTT CCT CTT CTT TTT CTT CTC C (**TS**) by $Ru(bpy)_3^{2+}$ was studied by cyclic voltammetry. This oligonucleotide forms either an intramolecular triplex, hairpin, or single strand, depending on the pH (Plum, G. E.; Breslauer, K. J. *J. Mol. Biol.* **1995**, *248*, 679–695). In the triplex form, the guanine doublet in **TS** is buried inside the folded structure, and as such is less susceptible to oxidation by electrogenerated $Ru(bpy)_3^{3+}$. Digital simulations of the catalytic voltammograms gave a rate constant of $3.5 \pm 0.2 \times 10^2$ M^{-1} s^{-1} for oxidation of the triplex form, while oxidation of the duplex and single-stranded forms occurred with much faster rate constants of $(3.5–9.1) \times 10^4$ M^{-1} s^{-1}. Experiments using a truncated form of **TS** that lacked the third strand of the triplex were consistent with these measurements. The $Ru(bpy)_3^{3+}$ complex was also generated by photolyzing $Ru(bpy)_3^{2+}$ in the presence of $Fe(CN)_6^{3-}$. This reaction produced strand scission following piperidine treatment, which was visualized using high-resolution gel electrophoresis. These experiments showed decreased reactivity for the triplex form, and also gave an unusual reversal of a common selectivity for the 5′-G of GG doublets generally seen in B-form DNA. This reversal was ascribed to strain caused by the location of the GG doublet adjacent to the hairpin loop.

Introduction

Three-stranded nucleic acid structures form when two DNA strands are hydrogen-bonded in the normal Watson−Crick duplex and a third strand forms Hoogsteen base pairs in the major groove.[1] The triple helix is thought to be involved in many biological processes due to the high occurrence of purine−pyrimidine tracts in eukaryotic and prokaryotic genomes.[2−4] Triplex DNA plays a role in the regulation of gene expression at the level of transcription by affecting promoter function.[5,6] Replication of DNA can be paused or inhibited by triplex formation,[7] an effect that can lead to a high degree of mutations.[5] Finally, triplex formation can also induce recombination events.[5,8] In antigene technology, oligonucleotides are designed to hybridize to specific double-stranded sequences in the chromosome to form triplexes, thereby inhibiting transcription and ultimately regulating the translation of specific proteins in the cell.[5,9−11] This process is similar to anti-sense technology that focuses on inhibition of translation through hybridization of an anti-sense strand to mRNA to form a duplex.[12,13]

Plum and Breslauer studied an intramolecular triplex (**TS**, Scheme 1) and, using spectroscopy and scanning differential calorimetry, created folding diagrams that indicate the structure of the nucleic acid strand under different temperature, pH, and ionic strength conditions.[14] The strand unfolds as the pH is raised, and the corresponding change in ionic strength also dictates conformation. Thermal denaturation studies at different pH levels revealed the various states.[14]

* Author to whom correspondence should be addressed. E-mail: holden@unc.edu.

(1) Blackburn, M. G.; Gait, M. J. *Nucleic Acids in Chemistry and Biology*; Oxford University Press: New York, 1996; p 18.
(2) Tiner, W. J.; Potaman, V. N.; Sinden, R. R.; Lyubchenko, Y. L. *J. Mol. Biol.* **2001**, *314*, 353−357.
(3) Bucher, P.; Yagil, G. *DNA Sequence* **1991**, *1*, 157−172.
(4) Behe, M. J. *Nucleic Acids Res.* **1995**, *23*, 689−695.
(5) Soyfer, V. N.; Potaman, V. N. *Triple-Helical Nucleic Acids*; Springer: New York, 1996.
(6) Lee, J. S.; Woodsworth, M. L.; Latimer, L. J. P.; Morgan, A. R. *Nucleic Acids Res.* **1984**, *12*, 6603−6614.
(7) Dayn, A.; Samadashwily, G. M.; Mirkin, S. M. *Proc. Natl. Acad. Sci. U.S.A.* **1992**, *89*, 11406−11410.
(8) Kohwi, Y.; Panchenko, Y. *Genes Dev.* **1993**, *7*, 1766−1778.
(9) Cooney, M.; Czernuszewicz, G.; Postel, E. H.; Flint, S. J.; Hogan, M. E. *Science* **1988**, *241*, 456−459.
(10) Maher, L. J.; Dervan, P. B.; Wold, B. *Biochemistry* **1992**, *31*, 70−81.
(11) Orson, F. M.; Thomas, D. W.; McShan, W. M.; Kessler, D. J.; Hogan, M. E. *Nucleic Acids Res.* **1991**, *19*, 3435−3441.
(12) Roth, C. M.; Yarmush, M. L. *Annu. Rev. Biomed. Eng.* **1999**, *1*, 265−297.
(13) Crooke, S. T. *Antisense Technol., Pt. A* **2000**, *313*, 3−45.

10.1021/ic049895x CCC: $27.50
Published on Web 07/13/2004

Scheme 1

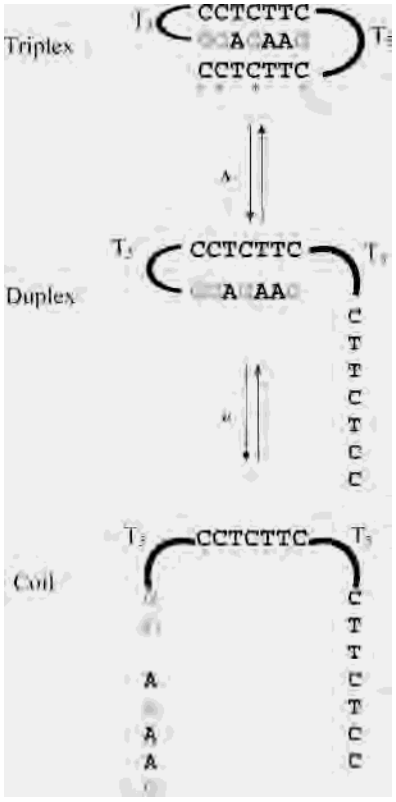

The same intramolecular triplex-forming folding oligonucleotide was used to test the abilities of a metal chemical nuclease ($Pt_2(pop)_4^{4-}$, pop = $P_2O_5H_2^{2-}$) to discern between the different folded or unfolded structures.[15] When photolyzed, the excited state of $Pt_2(pop)_4^{4-}$ damages DNA via 4′ and 5′ hydrogen abstraction; the extent of damage is controlled by the electrostatic repulsion of the two negatively charged species.[16] The DNA strand is then cleaved by piperidine treatment and visualized by gel electrophoresis, which results in a footprinting assay that reveals the protected and unprotected sites. The cleavage intensity data for **TS** with $Pt_2(pop)_4^{4-}$ were consistent with the melting curves at various pH levels as the temperature is increased.[15]

We report here the use of **TS** to test the effectiveness of detecting the different folded states of the nucleic acid strand using electrochemistry. Because guanine nucleobases reside on the inside of the fully folded structure, the different states can be distinguished based on the electrocatalytic reactivity of $Ru(bpy)_3^{3+}$ with guanine since this reaction is also based on solvent accessibility.[17] Thus, triplex state of **TS**, where the guanine nucleobases are occluded via formation of the folded structure, produced lower catalytic current, which was verified using photochemically generated Ru(III).

Experimental Section

Materials. Synthetic oligonucleotides were purchased from the Lineberger Comprehensive Cancer Center Nucleic Acids Core Facility and purified by gel electrophoresis on a 20% polyacrylamide gel with 7 M urea (USB). $[Ru(bpy)_3]Cl_2$ was synthesized according to published procedures.[18] Water was purified with a MilliQ purification system (Millipore).

Solution concentrations of metal complex or DNA were determined by spectrophotometry using a Cary 300 Bio UV−Visible scanning spectrophotometer. The extinction coefficient used for $Ru(bpy)_3^{2+}$ in water was $\epsilon_{452} = 14\,600\ M^{-1}cm^{-1}$.[19,20] Oligonucleotide strand concentrations were determined by absorbance at 260 nm with a previously determined extinction coefficient.[14] Double-stranded oligonucleotide solutions were prepared by mixing a 1:1.2 ratio of guanine-containing strand and its Watson−Crick complementary strand in sodium pyrophosphate buffer (10 mM $NaPP_i$, 800 mM NaCl, at various pH levels), heating at 90 °C for 5 min, and cooling to room temperature over 2 h.

Thermal Denaturation. Thermal denaturation experiments were performed on a Cary 300 Bio UV−Vis spectrophotometer. Oligonucleotide solutions contained 4 μM strand in 800 mM NaCl and 10 mM sodium pyrophosphate buffer at pH 4.8, 6.5, 7.0, and 8.0. Using the thermal melting program, the cell containing the quartz cuvette was preheated to 95 °C and then ramped from 95 to 5 °C and 5 to 95 °C at 0.5 °C/min. The absorbance at 260 nm was measured every 0.5 °C. The data were smoothed at 0.5 °C intervals with a filter of 5, and the derivative of the resulting curve was taken at a data interval of 0.5 °C to determine T_m. Experiments were performed in triplicate.

Electrochemistry. ITO electrodes were obtained from Delta Technologies, LTD (Stilwater, MN). All ITO electrodes were cleaned in a four-step sonication process involving an aqueous solution of Alconox, 2-propanol, and two washes with Milli-Q water (6 min each). Electrodes were then dried in an oven (90 °C) for 5 min. The freshly cleaned electrodes were used within 24 h. Experiments were performed on an EG&G PAR 273A potentiostat controlled by a PC. For cyclic voltammetry experiments, the electrode potential was scanned between 0.0 and 1.30 V. Each electrode was electrochemically conditioned prior to data collection by scanning the buffer solution at the intended scan rate (usually seven cycles). The background CV of sodium pyrophosphate buffer was subtracted from the subsequent metal and DNA CV data files before analysis. Experiments were performed in high-ionic-strength buffer solutions (10 mM sodium pyrophosphate and 800 mM NaCl). Cyclic voltammograms of 50 μM metal complex in the presence and absence of 25, 50, and 75 μM were recorded for each experiment.

Second-order rate constants were determined from the CV data (six CV files for each k_f value) by fitting with the DigiSim software package (BAS, West Lafayette, IN). Metal-only voltammograms were fit first to determine the effective electrode area (A, planar), heterogeneous electron-transfer rate constant between the metal complex and the electrode surface (k_s), and the homogeneous rate constant for the conversion of Ru^{3+} back to Ru^{2+}. The following parameters were required for fitting: $T = 298.15$ K, $R_U = 0$, $C_{DL} = 0$, and $\alpha = 0.5$. Diffusion coefficients used were 6×10^{-6} cm^2/s for $Ru(bpy)_3^{2+}$,[21] 1.5×10^{-6} cm^2/s for the oligonucleotide at pH

(14) Plum, G. E.; Breslauer, K. J. *J. Mol. Biol.* **1995**, *248*, 679−695.
(15) Ciftan, S. A.; Thorp, H. H. *J. Am. Chem. Soc.* **1998**, *120*, 9995−10000.
(16) Breiner, K. M.; Daugherty, M. A.; Oas, T. G.; Thorp, H. H. *J. Am. Chem. Soc.* **1995**, *117*, 11673−11679.
(17) Johnston, D. H.; Glasgow, K. C.; Thorp, H. H. *J. Am. Chem. Soc.* **1995**, *117*, 8933−8938.
(18) Kalyanasundaram, K. *Coord. Chem. Rev.* **1982**, *46*, 159−244.
(19) Turis, A. B., V.; Barigelletti, F.; Campagna, S.; Belser, P.; Zelewsky, A. V. *Coord. Chem. Rev.* **1988**, *84*, 85−277.
(20) Lumpkin, R. S. Analysis of processes controlling excited-state decay in polypyridyl complexes of Ru(II) and Os(II). University of North Carolina, Chapel Hill, 1987.
(21) Welch, T. W.; Corbett, A. H.; Thorp, H. H. *J. Phys. Chem.* **1995**, *99*, 11757−11763.

4.8, 1.25×10^{-6} cm^2/s at pH 6.5 and 7.0, and 1.0×10^{-6} cm^2/s at pH 8.0.[22,23] The mechanism used was as follows:

$$Ru^{3+} \rightarrow Ru^{2+} \quad (1)$$

$$Ru^{3+} + e^- \rightarrow Ru^{2+} \quad (2)$$

$$Ru^{3+} + DNA \rightarrow Ru^{2+} + DNA_{ox}\ (k_1) \quad (3)$$

$$Ru^{3+} + DNA_{ox} \rightarrow Ru^{2+} + DNA_{ox}'\ (k_2) \quad (4)$$

$$Ru^{3+} + DNA_{ox}' \rightarrow Ru^{2+} + DNA_{ox}''\ (k_3) \quad (5)$$

$$Ru^{3+} + DNA_{ox}'' \rightarrow Ru^{2+} + DNA_{ox}'''\ (k_4) \quad (6)$$

Concentration profiles for Ru^{2+} species were generated in SPECFIT using DigiSim values for k_1, k_2, k_3, k_4 and equal concentrations of Ru^{2+} and Ru^{3+}.[24] The resulting concentration profile was fit to the single bimolecular reaction, $Ru^{3+} + DNA \rightarrow Ru^{2+} + DNA_{ox}$ to yield k_f, also using the same concentrations for Ru.

Flash-Quench Experiments. Single-stranded oligonucleotide was 5′-radiolabeled using γ^{32}P-ATP (Perkin-Elmer). A 25-μL solution containing 1 μL of single-stranded oligonucleotide (5 μM), 5 μL of forward reaction buffer (5×), 1 μL of γ^{32}P-ATP, 1 μL of T4 polynucleotide kinase (Invitrogen), and 17 μL of MilliQ H_2O was heated in a water bath at 37 °C for 20 min. T4 Polynucleotide kinase was deactivated by heating the reaction solution at 65 °C for 10 min. The ^{32}P-labeled oligonucleotide (diluted to 50 μL) was then purified on a MicroSpin G-50 column (Amersham Pharmacia Biotech). The resulting ^{32}P-labeled oligonucleotide was ethanol-precipitated and resuspended in MilliQ water (~300 K cts/5 μL).

Radiolabeled double-stranded oligonucleotide solutions were prepared by mixing a 1:1.2 ratio of unlabeled oligonucleotide and complementary oligonucleotide (20 μM stock solutions) in 10 mM sodium pyrophosphate buffer ($NaPP_i$), 800 mM NaCl (at pH 4.8, 6.5, 7.0, and 8.0). ^{32}P-labeled oligonucleotide (5 μL, 300 K cts) was added to each 20-μL reaction solution. The resulting mixture was heated to 90 °C for 5 min and cooled to room temperature over 2 h to anneal the strands. Hybridized ^{32}P-labeled oligonucleotide (20 μL) was combined with 20 μL of prepared stock solutions of either buffer only (10 mM $NaPP_i$ buffer, 800 mM NaCl), 100 μM $Ru(bpy)_3^{2+}$, 50 μM $Ru(bpy)_3^{2+}$ and 500 μM $Fe(CN)_6^{3-}$, or 100 μM $Ru(bpy)_3^{2+}$ and 1 mM $Fe(CN)_6^{3-}$ to yield a total reaction solution (40 μL) consisting of 10 μM oligonucleotide. All reactions were carried out at pH 4.8, 6.5, 7.0, and 8.0. In a polyspring insert tube (National Scientific Company), the reaction solution was photolyzed for 10 min with a 300-W Hg Lamp (Oriel) and a monochromator set to 368 nm (60% transmission, 40 nM fwhm). Following photolysis, the reactions were quenched with 8 μL of 0.8 M EDTA and ethanol precipitated with ammonium acetate as described elsewhere.[25] Samples were treated with piperidine prior to denaturing gel electrophoresis.[25]

All samples were pelleted by centrifugation at 16 000*g* for 20 min, resuspended in 12 μL of gel loading dye solution (80% formamide, 0.5 X TBE buffer, and orange G dye), and heated at 90 °C for 5 min. Each sample (6 μL) was loaded into a well of 20% denaturing polyacrylamide gel containing 7 M urea and run at 35 W for 2 h. The gel was then transferred to a phosphorimaging screen, exposed overnight, and scanned on a Storm 840 system phosphorimager (Molecular Dynamics).

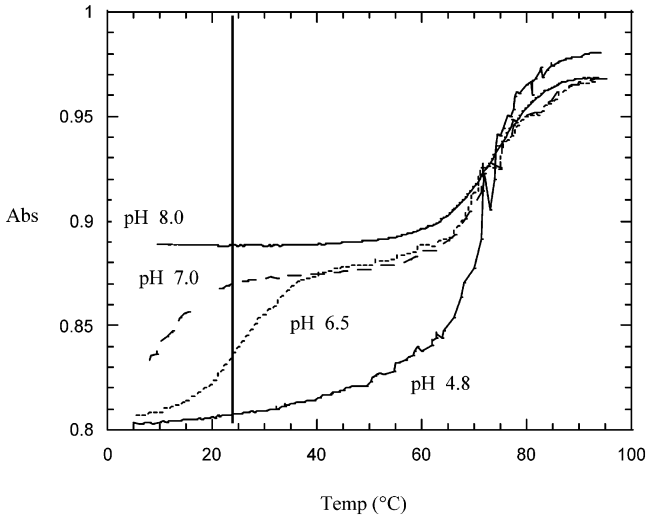

Figure 1. Thermal denaturation experiment for **TS** at pH 4.8 (solid line, bottom), $T_m = 70.1 \pm 0.9$ °C; pH 6.5 (dotted line), $T_m = 27.0 \pm 0.9$ °C, 71.0 ± 0.9 °C; pH 7.0 (dashed line), $T_m = 10.1 \pm 0.5$ °C, 70.4 ± 0.9 °C; pH 8.0 (solid line, top), $T_m = 73.3 \pm 0.9$ °C. Solid vertical line denotes room temperature.

Table 1. Sequences of Nucleic Acid Strands Examined in This Study

strand name	sequence (**5′−3′**)
TS	GAA GAG GTT TTT CCT CTT CTT TTT CTT CTC C
HP	GAA GAG GTT TTT CCT CTT C
TS·C	**TS** hybridized to its complement

Results and Discussion

Oligonucleotide Characterization. The strand forming an intramolecular triplex (**TS**, sequences given in Table 1) was originally studied by Plum and Breslauer and was shown to exist in three different conformations, depending on the pH and salt concentration of the solution.[14] These states are shown in Scheme 1 and were confirmed by thermal denaturation (Figure 1). At room temperature (indicated by the vertical solid line in Figure 1), the strand is a triplex at pH 4.8, is in equilibrium between the duplex and triplex structures at pH 6.5, is a duplex at pH 7.0, and is nearly all duplex at pH 8.0. We also synthesized the related nucleic acid strand **HP**, which only forms the first hairpin loop structure because it lacks the tail arm on the 3′ end. This structure denatures at about 68 °C, independent of the pH (data not shown); the m-fold program predicts a denaturation temperature of 71 °C.[26] The thermal denaturation curve obtained is similar to that for **TS** at high pH. Also, when the **TS** sequence was hybridized to its complement to form **TS·C**, the duplex denatured at roughly 75 °C, consistent with the predicted melting temperature of 77 °C.[27]

Electrochemistry. The guanine nucleotides of **TS** are buried in the middle of the structure when folded into the

(22) Tirado, M. M.; DeLatorre, J. G. *J. Chem. Phys.* **1980**, *73*, 1986−1993.
(23) Tirado, M. M.; Martinez, C. L.; DeLatorre, J. G. *J. Chem. Phys.* **1984**, *81*, 2047−2052.
(24) Weatherly, S. C. The Mechanism of Metal-Mediated Guanine Oxidation in Native and Non-Native DNA Environments. University of North Carolina, Chapel Hill, 2000.
(25) Sambrook, J. F., E. F.; Maniatis, T. *Molecular Cloning: A laboratory manual*. 2nd Cold Spring Harbor Press: New York, 1989.
(26) Zuker, M. http://www.bioinfo.rpi.edu/applications/mfold/old/dna/form1.cgi (July 30, 2001).
(27) Blake, R. D.; Delcourt, S. G. *Nucleic Acids Res.* **1998**, *26*, 3323−3332.

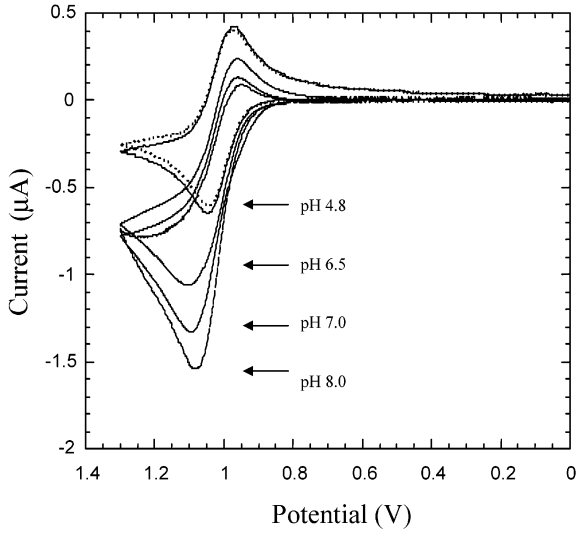

Figure 2. Cyclic voltammogram of 50 μM $Ru(bpy)_3^{2+}$ in the absence (dotted line) and presence (solid lines) of 25 μM [G] **TS** at pH 4.8, 6.5, 7.0, and 8.0 in 10 mM $NaPP_i$ buffer and 800 mM NaCl at 25 mV/s.

triplex conformation but can also be in duplex or single-stranded form, depending on the pH and corresponding structure (Scheme 1). Because the rate of electrocatalytic oxidation increases with solvent accessibility,[17] we expected that there would be a change in the amount of catalytic current observed from the reaction of $Ru(bpy)_3^{3+}$ with guanine in the nucleic acid strand depending on the structure. Cyclic voltammetry experiments were therefore performed on **TS** in the presence of $Ru(bpy)_3^{2+}$. As predicted, the amount of catalytic current observed increased as the pH increased (Figure 2). At pH 4.8, when the nucleic acid is mostly in the triplex conformation, no catalysis was observed, indicating that electron transfer is inhibited. As the pH was further increased, the strand unfolded, and catalysis from guanine oxidation was observed.

Several reactions were performed to verify that the reactivity trend in Figure 2 resulted from the structural changes in the conformation of the nucleic acid strand and not solely from an effect of the pH itself on the innate guanine−Ru(III) reaction. Cyclic voltammetry experiments on the folded hairpin **HP** did in fact produce an increase in observed current as the pH was increased (Figure 3), and similar results were obtained for electrochemistry reactions with **TS·C** (Figure 4). We have shown that the guanine−Ru(III) electron transfer proceeds via a proton-coupled pathway, where the abstraction of an electron from guanine occurs concomitantly with deprotonation.[28] This process becomes more facile as the pH is increased, which apparently gives some increase in catalytic current. However, the increase shown in Figures 3 and 4 is not as dramatic as that seen with **TS** in Figure 2.

Rate constants for these oxidation reactions were determined by simulating the cyclic voltammograms using the DigiSim program and methods we have developed in our laboratory.[29,30] The resulting values (Table 2) were independent of scan rate and substrate concentration, and the trend follows that of the observed current enhancements. As expected, **HP** is oxidized 43 times faster at pH 4.8 than **TS**.

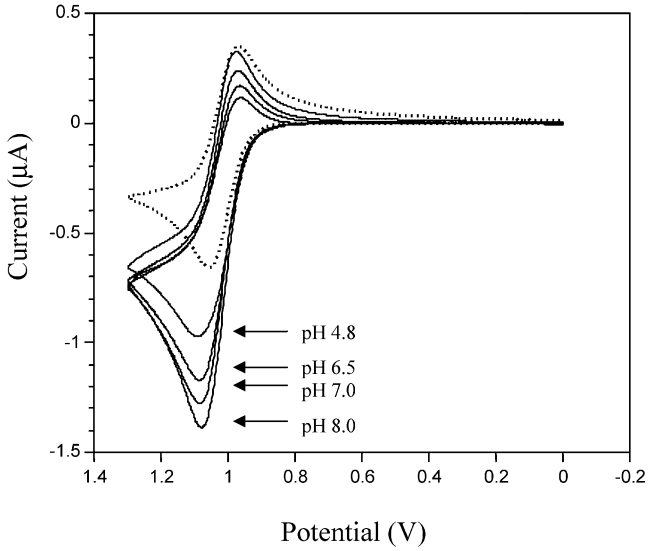

Figure 3. Cyclic voltammogram of 50 μM $Ru(bpy)_3^{2+}$ in the absence (dotted line) and presence (solid lines) of 25 μM [G] **HP** at pH 4.8, 6.5, 7.0, and 8.0 in 10 mM $NaPP_i$ buffer and 800 mM NaCl at 25 mV/s.

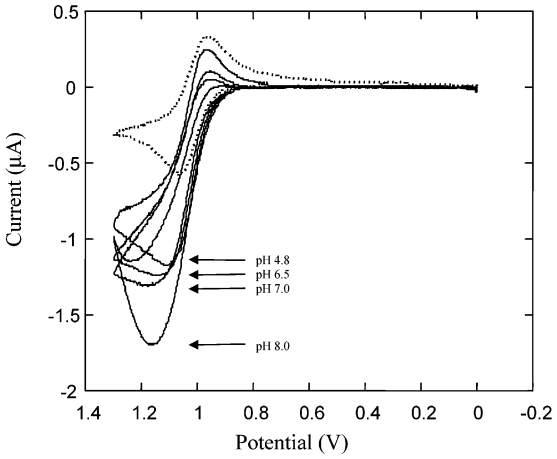

Figure 4. Cyclic voltammogram of 50 μM $Ru(bpy)_3^{2+}$ in the absence (dotted line) and presence (solid lines) of 25 μM [G] **TS·C** at pH 4.8, 6.5, 7.0, and 8.0 in 10 mM $NaPP_i$ buffer and 800 mM NaCl at 25 mV/s.

Table 2. Second-Order Rate Constants for Guanine Oxidation by $Ru(bpy)_3^{2+}$ (Substrate Concentration Range from 10 to 50 μM and Scan Rates from 25 to 250 mV/s)

pH	k_f, **TS** ($M^{-1}s^{-1}$)	k_f, **HP** ($M^{-1}s^{-1}$)	k_f, **TS·C** ($M^{-1}s^{-1}$)
4.8	$3.5 \pm 0.2 \times 10^2$	$1.5 \pm 0.9 \times 10^4$	$4.3 \pm 0.2 \times 10^4$
6.5	$3.5 \pm 0.7 \times 10^4$	$4.1 \pm 0.3 \times 10^4$	$4.8 \pm 0.8 \times 10^4$
7.0	$5.2 \pm 0.6 \times 10^4$	$5.9 \pm 0.5 \times 10^4$	$5.9 \pm 0.2 \times 10^4$
8.0	$9.1 \pm 0.7 \times 10^4$	$9.0 \pm 0.9 \times 10^4$	$2.4 \pm 0.9 \times 10^5$

Also, the oxidation rate is increased by 2 orders of magnitude from pH 4.8 to 6.5 as the triplex unfolds to the hairpin. The rate constants at higher pH fall within the range of those observed in a number of sequence contexts.[31,32]

Two factors, therefore, likely lead to inhibition of electron transfer in the **TS** form. First, the 3′ tail of the strand of the

(28) Weatherly, S. C.; Yang, I. V.; Thorp, H. H. *J. Am. Chem. Soc.* **2001**, *123*, 1236−1237.
(29) Weatherly, S. C. Mechanism of Metal-Mediated Guanine Oxidation in Native and Non-Native DNA Environments. University of North Carolina, Chapel Hill, 2001.
(30) Sistare, M. F.; Holmberg, R. C.; Thorp, H. H. *J. Phys. Chem. B* **1999**, *103*, 10718−10728.

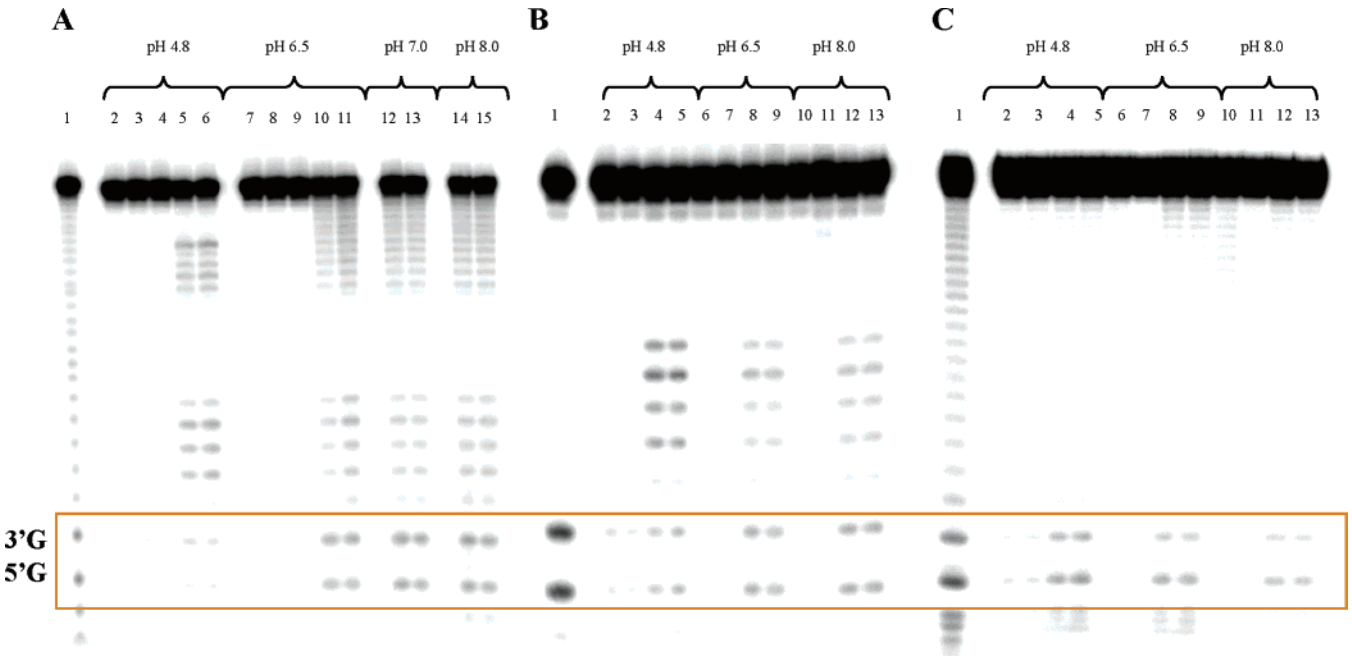

Figure 5. Flash-quench reaction for **1** with **TS** (A), **HP** (B), and **TS·C** (C). (A) Lane 1 Maxam−Gilbert G-lane; pH 4.8; lane 2 = 10 μM DNA (no irradiation); lane 3 = lane 2 (irradiated); lane 4 = lane 2 + 50 μM $Ru(bpy)_3^{2+}$ (no irradiation); lane 5 = lane 2 + 25 μM $Ru(bpy)_3^{2+}$ + 250 μM $Fe(CN)_6^{3-}$ (irradiated); lane 6 = lane 2 + 50 μM $Ru(bpy)_3^{2+}$ + 500 μM $Fe(CN)_6^{3-}$ (irradiated); lanes 7−11 = lanes 2−6 at pH 6.5; lanes 12,13 = lanes 5,6 at pH 7.0; lanes 14,15 = lanes 5,6 at pH 8.0. (B) Lane 1 Maxam−Gilbert G-lane; pH 4.8; lane 2 = 10 μM DNA (irradiated); lane 3 = lane 2 + 50 μM $Ru(bpy)_3^{2+}$ (no irradiation); lane 4 = lane 2 + 25 μM $Ru(bpy)_3^{2+}$ + 250 μM $Fe(CN)_6^{3-}$ (irradiated); lane 5 = lane 2 + 50 μM $Ru(bpy)_3^{2+}$ + 500 μM $Fe(CN)_6^{3-}$ (irradiated); lanes 6−9 = lanes 2−5 at pH 6.5; lanes 10−13 = lanes 2−5 at pH 8.0. (C) Lane 1 Maxam−Gilbert G-lane; pH 4.8; lane 2 = 10 μM DNA (irradiated); lane 3 = lane 2 + 50 μM $Ru(bpy)_3^{2+}$ (no irradiation); lane 4 = lane 2 + 25 μM $Ru(bpy)_3^{2+}$ + 250 μM $Fe(CN)_6^{3-}$ (irradiated); lane 5 = lane 2 + 50 μM $Ru(bpy)_3^{2+}$ + 500 μM $Fe(CN)_6^{3-}$(irradiated); lanes 6−9 = lanes 2−5 at pH 6.5; lanes 10−13 = lanes 2−5 at pH 8.0. All in 10 mM $NaPP_i$ buffer and 800 mM NaCl.

triplex is folded into the major groove of the DNA, inhibiting access of $Ru(bpy)_3^{3+}$ to the buried guanines; we have similarly observed protection of guanine from $Ru(bpy)_3^{3+}$ in a number of highly folded structures with both $Ru(bpy)_3^{2+}$ and $Ru(tpy)(bpy)O^{2+}$, which is also a solution-bound oxidant (tpy = 2,2′,2″-terpyridine). Furthermore, the protonation of cytosine nucleobases that accompanies triplex formation probably draws electron density through the hydrogen bond from guanine to cytosine, resulting in a less electron-rich guanine that is more difficult to oxidize. A combination of these two factors likely reduces the rate of electron transfer from triplex guanines to the oxidizing metal complex.

Flash-Quench Photochemistry. The guanine−$Ru(bpy)_3^{3+}$ reaction was also monitored using the flash-quench reaction, where the oxidized metal is photochemically generated by photolyzing $Ru(bpy)_3^{2+}$ in the presence of $Fe(CN)_6^{3-}$. The photogenerated $Ru(bpy)_3^{3+}$ reacts with guanine in the nucleic acid strand to produce piperidine-labile lesions.[33,34] Analysis of the generated DNA fragments by high-resolution gel electrophoresis allows visualization of the sites of electron transfer, and the trends in observed cleavage intensities typically parallel the observed electron-transfer rates from electrochemistry.

Figure 5A shows the sites of oxidation as a function of pH produced by photolysis of **TS** with $Ru(bpy)_3^{2+}$ and $Fe(CN)_6^{3-}$. Note that oxidation of the guanines near the end of the strand could not be assessed due to technical constraints on the difficulty of studying end nucleotides; rather, our analysis focuses on the adjacent guanines near the hairpin loop. As expected, no reactivity was observed in the absence of quencher (lanes 4) or light (lane 2), or upon photolysis of **TS** in buffer alone (lane 3). Control reactions at pH 7.0 and 8.0 yielded results similar to those at pH 6.5 (data not shown). The oxidation of guanine is barely detectable at pH 4.8 while the other pH values show considerable reactivity that is essentially independent of pH. A similar lack of reactivity in triplexes was observed independently by Barton et al. and Schuster et al. for long-range guanine electron transfer.[35−37] The **HP** sequence, which cannot form the triplex, does not exhibit significant variation in guanine oxidation upon varying the pH, as expected (Figure 5B). A slight increase in reactivity was observed in the lanes containing a higher concentration of Ru^{3+}.

Effect on Oxidation of Guanine Doublets. When two adjacent guanines are present in a DNA sequence, the 5′-guanine is generally oxidized preferentially by one-electron agents in normal duplex DNA.[38,39] This effect is typically

(31) Johnston, D. H.; Thorp, H. H. *J. Phys. Chem.* **1996**, *100*, 13837−13843.
(32) Sistare, M. F.; Codden, S. J.; Heimlich, G.; Thorp, H. H. *J. Am. Chem. Soc.* **2000**, *122*, 4742−4749.
(33) Szalai, V. A.; Thorp, H. H. *J. Am. Chem. Soc.* **2000**, *122*, 4524−4525.
(34) Stemp, E. D. A.; Arkin, M. R.; Barton, J. K. *J. Am. Chem. Soc.* **1997**, *119*, 2921−2925.
(35) Nunez, M. E.; Noyes, K. T.; Gianolio, D. A.; McLaughlin, L. W.; Barton, J. K. *Biochemistry* **2000**, *39*, 6190−6199.
(36) Kan, Y. Z.; Schuster, G. B. *J. Am. Chem. Soc.* **1999**, *121*, 11607−11614.
(37) Frier, C.; Mouscadet, J. F.; Decout, J. L.; Auclair, C.; Fontecave, M. *Chem. Commun.* **1998**, 2457−2458.

observed for radiolabeled oligonucleotides after reaction with one-electron oxidants followed by piperidine treatment. Visualization of the fragments by high-resolution gel electrophoresis then reveals more intense bands at the 5′-guanine of the GG doublet. For triplexes, the oxidation of GG doublets was studied in an *intermolecular* triplex by Schuster and co-workers.[36] In this study, anthraquinone was covalently attached to the 5′ end of the third strand and irradiated to study charge transport at long range through the DNA helix. As described above, these studies showed generally lower damage in the triplex regions and a reversed preference in the GG doublet where the 3′G was favored over the 5′G in the triplex form.[36] Similar behavior was observed for reaction of the *intramolecular* triplex (**TS**) with $Ru(bpy)_3^{3+}$ at pH 4.8 (Figure 5A). The average ratio of cleavage intensities at the 5′-G to 3′-G was 0.73 ± 0.04 for Figure 5A at pH 4.8.

To understand whether the reversed specificity observed for the **TS** was due to formation of the triplex, we examined the cleavage of the GG doublets in the **HP** sequence. Surprisingly, the **HP** sequence does not exhibit characteristic 5′ reactivity over the pH range. Instead, both guanine sites in the GG stack show equal extent of reaction (Figure 5B). The average ratio of intensities for the 5′-G to 3′-G in Figure 5B was 1.00 ± 0.05. These guanines are located adjacent to the hairpin loop, which could strain the 3′GC pair, disrupt favorable alignment of the heteroatoms in the two nucleobases,[38,39] and shift electron density away from the 5′G. The reactivity of **HP** is similar to that of the duplex form of **TS** at higher pH (above 4.8). The average ratio of intensities for the 5′-G to 3′-G in Figure 5A above pH 4.8 was 0.97 ± 0.03. However, when the **TS** sequence is hybridized to its complement (**TS·C**), the preferential reactivity at the 5′-guanine is restored (Figure 5C). As with **HP**, the reaction of **TS·C** is independent of pH; the average ratio of intensities for cleavage at 5′-G to 3′-G was 1.33 ± 0.04 in Figure 5C.

Conclusions

The oligonucleotide **TS** developed by Plum and Breslauer allows study of triplex, duplex and single-stranded DNA in a single sequence.[14] We showed previously that the abstraction of hydrogen atoms from the sugar residues of **TS** by $Pt_2(pop)_4^{4-}$ was modulated by the pH and temperature effects on the structure.[15] Here, we demonstrate that the electrocatalytic oxidation of internal guanines by $Ru(bpy)_3^{3+/2+}$ is impeded in the triplex form, producing a decrease in catalytic current. This decrease is consistent with a low reactivity in photochemical oxidations visualized by high-resolution gel electrophoresis. These latter experiments show a reversal in the preferential oxidation of the 5′-G of GG doublets normally seen in duplex DNA.[38,39] Because this reversed selectivity is also observed in the duplex hairpin form but not when **TS** is hybridized to its complete Watson−Crick complement, we ascribe this change in selectivity to strain induced by the nearby hairpin loop of the duplex.

Acknowledgment. This research was sponsored by Xanthon, Inc. R.C.H. thanks the Department of Education for a fellowship.

IC049895X

(38) Prat, F.; Houk, K. N.; Foote, C. S. *J. Am. Chem. Soc.* **1998**, *120*, 845−846.
(39) Sugiyama, H.; Saito, I. *J. Am. Chem. Soc.* **1996**, *118*, 7063−7068.